Multiple Label-Free Detection of Antigen–Antibody Reaction Using Localized Surface Plasmon Resonance-Based Core–Shell Structured Nanoparticle Layer Nanochip

ARTICLE *in* ANALYTICAL CHEMISTRY · OCTOBER 2006

Impact Factor: 5.64 · DOI: 10.1021/ac0608321 · Source: PubMed

8 AUTHORS, INCLUDING:

Naoki Nagatani

Okayama University of Science

47 PUBLICATIONS **1,476** CITATIONS

SEE PROFILE

Anal. Chem. **2006,** *78,* 6465−6475

Multiple Label-Free Detection of Antigen−Antibody Reaction Using Localized Surface Plasmon Resonance-Based Core−Shell Structured Nanoparticle Layer Nanochip

Tatsuro Endo,[†] Kagan Kerman,[‡] Naoki Nagatani,[⊥] Ha Minh Hiepa,[‡] Do-Kyun Kim,[‡] Yuji Yonezawa,[§] Koichi Nakano,[§] and Eiichi Tamiya*,[‡]

Department of Mechano-Micro Engineering, Interdisciplinary Graduate School of Science and Engineering, Tokyo Institute of Technology, 4259 Nagatsuta-cho, Midori-ku, Yokohama, 226-8502, Japan, School of Materials Science, Japan Advanced Institute of Science and Technology (JAIST) 1-1, Asahidai, Nomi City, Ishikawa, 923-1292, Japan, Industrial Research Institute of Ishikawa, 2-1 Kuratsuki, Kanazawa City, Ishikawa 920-8203, Japan, and Department of Biotechnology and Applied Chemistry, Faculty of Engineering, Okayama University of Science, 1-1 Ridai-cho, Okayama 700-0005, Japan

In this research, a localized surface plasmon resonance (LSPR)-based bioanalysis method for developing multiarray optical nanochip suitable for screening bimolecular interactions is described. LSPR-based label-free monitoring enables to solve the problems of conventional methods that require large sample volumes and time-consuming labeling procedures. We developed a multiarray LSPR-based nanochip for the label-free detection of proteins. The multiarray format was constructed by a core−shell-structured nanoparticle layer, which provided 300 nanospots on the sensing surface. Antibodies were immobilized onto the nanospots using their interaction with Protein A. The concentrations of antigens were determined from the peak absorption intensity of the LSPR spectra. We demonstrated the capability of the array measurement using immunoglobulins (IgA, IgD, IgG, IgM), C-reactive protein, and fibrinogen. The detection limit of our label-free method was 100 pg/mL. Our nanochip is readily transferable to monitor the interactions of other biomolecules, such as whole cells or receptors, with a massively parallel detection capability in a highly miniaturized package. We anticipate that the direct label-free optical immunoassay of proteins reported here will revolutionize clinical diagnosis and accelerate the development of hand-held and user-friendly point-of-care devices.

The post-genome era of life sciences is rapidly moving beyond functional genomics to proteomics.[1] Since genome sequencing has evolved to become a routine technology, many efforts have been in progress to improve the proteomics technologies.[2] As an emerging field in life sciences, proteomics is not only based on, but also being developed beyond, genomics. However, a large-scale, rapid, and ultrasensitive assay system is highly desired. The large-scale and partly high-throughput characterization of the human proteome has become possible with the sophisticated biochemical techniques. Although enzyme-linked immunosorbent assay and two-dimensional gel electrophoresis are currently the most widely used bioanalysis tools for monitoring protein−protein interactions, they bring along disadvantages with regard to throughput, reproducibility, and sensitivity.[3] Surface plasmon resonance (SPR) is a strong alternative to the existing technologies for monitoring the biomolecular interactions. Unfortunately, conventional SPR reflectometry requires sophisticated optical instrumentation associated with the detection system. This latter limitation is significant, because biochips are urgently in demand for high-throughput and cost-effective monitoring. To overcome these disadvantages of conventional detection systems, biochip assay systems employing micro and nano electromechanical systems (MEMS and NEMS) have been developed.[4] A highly developing trend in the application of MEMS and NEMS technologies in life sciences and biotechnology is directed toward miniaturization and multidetection. These chip technologies have several advantages over the conventional bioanalysis systems. First, the chip-based assays enable rapid analysis of a large number of samples in a single experiment. Second, the amount of material required is significantly small. Reaction volumes are lower than the amount that is typically used in conventional microtiter plates. Third, the signal-to-noise ratio exhibited by micro or nano- fabricated biochips is much better than that observed for conventional microtiter plate assay systems.[5,6] In addition to the advantages, such as the reduced reagent consumption and the laboratory space conservation, lab-on-a-chip technology offers new prospects for laboratory innovation and automation. Biochips

* Corresponding author. E-mail: tamiya@jaist.ac.jp.
[†] Tokyo Institute of Technology.
[‡] JAIST.
[§] Industrial Research Institute of Ishikawa.
[⊥] Okayama University of Science.

(1) Drewes, G.; Bouwmeester, T. *Curr. Opin. Cell Biol.* **2003**, *15*, 199−205.
(2) Timperman, A. T.; Aebersold, R. *Anal. Chem.* **2000**, *72*, 4115−4121.
(3) Petach, H.; Gold, L. *Curr. Opin. Biotechnol.* **2002**, *13*, 309−314.
(4) Talapatra, A.; Rouse, R.; Hardiman, G. *Pharmacogenomics* **2002**, *3*, 527−536.
(5) Workman, J., Jr.; Koch, M.; Veltkamp, D. *Anal. Chem.* **2005**, *77*, 3789−3806.
(6) Gardeniers, H.; Van Den Berg, A. *Int. J. Environ. Anal. Chem.* **2004**, *84*, 809−819.

10.1021/ac0608321 CCC: $33.50
Published on Web 07/22/2006

in proteomics have evolved into powerful tools for quantifying proteins and qualifying their state of activation in complex biological samples. Until now, several kinds of biochips for proteomics using MEMS and NEMS technologies have been developed, such as an array-based[7−9] and a microfluidic biochip.[10−13] However, these biochips require the labeling of the proteins with different types of reagents, such as fluorescent dyes or enzymes. The labeling procedure with these reagents is a difficult and time-consuming task and may cause an inhibition on the biofunctions of the native protein. To overcome these disadvantages, we developed a novel localized surface plasmon resonance (LSPR)-based nanochip for label-free monitoring of biorecognition events.

LSPR is currently of considerable interest in the fabrication and optical characterization of gold and silver nanoparticles on solid supports.[14,15] Gold and silver nanoparticles are subject to active research because of their well-documented or proposed importance in various nano-optical applications, such as biochips,[16−19] and a nanoruler.[20] LSPR-based monitoring methods can detect an immediate increase in thickness of a biomolecular layer caused by the reaction between the solution component under study and the receptor layer immobilized on the surface.[21,22] The specific optical properties originate from LSPR, a class of surface modes that involves the collective excitation of conduction electrons in response to an incident electromagnetic field. It is known that nanoparticles, such as gold and silver, possess strong absorption in the visible region, often coined as localized surface plasmon absorption. Such LSPR occurs when the incident photon frequencies match the collective oscillations of the conduction electrons of metal nanoparticles or metal islands. The particles in the nanoscale exhibit unique optical responses within the UV−vis region,[23,24] where the absorbance shows an exponential decay with decreasing photon energy (the so-called Mie scattering), onto which an LSPR band, specific for the particle material, is superimposed. The surface plasmon energy and intensity have been found to be sensitive to a number of factors, including particle conformation, immediate surrounding media, etc.[25−30] In addition, the LSPR-based device can be constructed with a simple optical system. Commercial SPR sensing devices generally operate in total internal reflection mode using the Kretschmann configuration. However, our LSPR-based nanochip can operate in transmission geometry, which has already been established for ultrathin gold island films, and gold or silver nanoparticles immobilized on glass.[31−36] Thus, we fabricated a core−shell structured nanoparticle layer substrate that can be utilized as an LSPR-based nanochip. Our nanochip also operates in transmission mode, allowing for a simpler collinear optical arrangement while providing a smaller probing area than the typical Kretschmann configuration. Since the sensing capability of LSPR-based methods can be tuned by changing the shape, size, and material composition of the nanoparticles,[31] we obtained ultrasensitivity and selectivity against target proteins by using our novel nanoconfiguration.

Previously, we achieved the label-free detection of the antigen−antibody reactions,[37] peptide nucleic acid (PNA)-DNA, and DNA−DNA hybridization[38] using our LSPR-based nanochip. As a result, promising performance of our LSPR-based nanochip could be observed. On the basis of the characteristics of our previous chips, we fabricated the multiarray LSPR-based nanochip for the multiple detection of the six different proteins in this report.

With the significant advances in microfabrication technology, biochips for the parallel detection of multiple target molecules have been developed using several detection principles, such as surface plasmon resonance,[39,40] electrochemistry[41,42] and faradic impedance spectroscopy.[43] Functionalized cantilever arrays also provided a promising platform for label-free detection of biomolecules.[44] Our LSPR-based nanochip provides a highly sensitive and promising alternative to the existing devices in a compact package with a simple optical instrumentation.

(7) Zhi, Z. L.; Murakami, Y.; Morita, Y.; Hasan, Q.; Tamiya, E. *Anal. Biochem.* **2003**, *318*, 236−243.
(8) Matsubara, Y.; Kerman, K.; Kobayashi, M.; Yamamura, S.; Morita, Y.; Takamura, Y.; Tamiya, E. *Anal. Chem.* **2004**, *76*, 6434−6439.
(9) Matsubara, Y.; Kerman, K.; Kobayashi, M.; Yamamura, S.; Morita, Y.; Tamiya, E. *Biosens. Bioelectron.* **2005**, *20*, 1482−1490.
(10) Murakami, Y.; Endo, T.; Yamamura, S.; Nagatani, N.; Takamura, Y.; Tamiya, E. *Anal. Biochem.* **2004**, *334*, 111−116.
(11) Endo, T.; Okuyama, A.; Matsubara, Y.; Nishi, K.; Kobayashi, M.; Yamamura, S.; Morita, Y.; Takamura, Y.; Mizukami, H.; Tamiya, E. *Anal. Chim. Acta* **2005**, *531*, 7−13.
(12) Matsubara, Y.; Murakami, Y.; Kobayashi, M.; Morita, Y.; Tamiya, E. *Biosens. Bioelectron.* **2004**, *19*, 741−747.
(13) Shaikh, K. A.; Ryu, K. S.; Goluch, E. D.; Nam, J. M.; Liu, J.; Thaxton, C. S.; Chiesl, T. N.; Barron, A. E.; Lu, Y.; Mirkin, C. A.; Liu, C. *Proc. Natl. Acad. Sci. U.S.A.* **2005**, *102*, 9745−9750.
(14) Love, J. C.; Estroff, L. A.; Kriebel, J. K.; Nuzzo, R. G.; Whitesides, G. M. *Chem. Rev.* **2005**, *105*, 1103−1169.
(15) Hutter, E.; Fendler, J. H. *Chem. Commun.* **2002**, 378−379.
(16) Haes, A. J.; Van Duyne, R. P. *J. Am. Chem. Soc.* **2002**, *124*, 10596−10604.
(17) Frederix, F.; Friedt, J. M.; Choi, K. H.; Laureyn, W.; Campitelli, A.; Mondelaers, D.; Maes, G.; Borghs, G. *Anal. Chem.* **2003**, *75*, 6894−6900.
(18) Nath, N.; Chilkoti, A. *J. Fluoresc.* **2004**, *14*, 377−389.
(19) Stuart, D. A.; Yonzon, C. R.; Zhang, X.; Lyandres, O.; Shah, N. C.; Glucksberg, M. R.; Walsh, J. T.; Van Duyne, R. P. *Anal. Chem.* **2005**, *77*, 4013−4019.
(20) Sönnichsen, C.; Reinhard, B. M.; Liphardt, J.; Alivisatos, A. P. *Nat. Biotechnol.* **2005**, *23*, 741−745.
(21) Haes, A. J.; Chang, L.; Klein, W. L.; Van Duyne, R. P. *J. Am. Chem. Soc.* **2005**, *127*, 2264−2271.
(22) Himmelhaus, M.; Takei, H. *Sens. Actuators, B* **2000**, *63*, 24−30.
(23) Jin, R.; Cao, Y.; Mirkin, C. A.; Kelly, K. L.; Schatz, G. C.; Zheng, J. G. *Science* **2001**, *294*, 1901−1903.
(24) Prodan, E.; Nordlander, P.; Halas, N. J. *Nano Lett.* **2003**, *3*, 1411−1415.
(25) Haes, A. J.; Zou, S.; Schatz, G. C.; Van Duyne, R. P. *J. Phys. Chem. B* **2004**, *108*, 6961−6968.
(26) Haes, A. J.; Zou, S.; Schatz, G. C.; Van Duyne, R. P. *J. Phys. Chem. B* **2004**, *108*, 109−116.
(27) Yonzon, C. R.; Jeoung, E.; Zou, S.; Schatz, G. C.; Mrksich, M.; Van Duyne, R. P. *J. Am. Chem. Soc.* **2004**, *126*, 12669−12676.
(28) Hong, X.; Kao, F. J. *Appl. Opt.* **2004**, *43*, 2868−2873.
(29) Nath, N.; Chilkoti, A. *Anal.Chem* **2004**, *76*, 5370−5378.
(30) Underwood, S.; Mulvaney, P. *Langmuir* **1994**, *10*, 3427−3430.
(31) Prasad, N. P. In *Nanophotonics*, John Wiley & Sons: New York, 2004; p 129−151.
(32) Hutter, E.; Fendler, J. H. *Chem. Commun.* **2002**, 378−379.
(33) Haes, A. J.; Van Duyne, R. P. *Anal. Bioanal. Chem.* **2004**, *379*, 920−930.
(34) Nath, N.; Chilkoti, A. *Anal. Chem.* **2002**, *74*, 504−509.
(35) Haes, A. J.; Stuart, D. A.; Nie, S.; Van Duyne, R. P. *J. Fluoresc.* **2004**, *14*, 355−367.
(36) Liz-Marzán, L. M.; Giersig, M.; Mulvaney, P. *Langmuir* **1996**, *12*, 4329−4335.
(37) Endo, T.; Yamamura, S.; Nagatani, N.; Morita, Y.; Takamura, Y.; Tamiya, E. *Sci. Technol. Adv. Mater.* **2005**, *6*, 491−500.
(38) Endo, T.; Kerman, K.; Nagatani, N.; Takamura, Y.; Tamiya, E. *Anal. Chem.* **2005**, *77*, 6976−6984.
(39) Wegner, G. J.; Lee, H. J.; Corn, R. M. *Anal. Chem.* **2002**, *74*, 5161−5168.
(40) Safsten, P.; Klakamp, S. L.; Drake, A. W.; Karlsson, R.; Myszka, D. G. *Anal. Biochem.* **2006**, *353*, 181−190.
(41) Wilson, M. S.; Nie, W. *Anal. Chem.* **2006**, *78*, 2507−2513.
(42) Goral, V. N.; Zaytseva, N. V.; Baeumner, A. J. *Lab Chip* **2006**, *6*, 414−421.
(43) Yu, X.; Lv, R.; Ma, Z.; Liu, Z.; Hao, Y.; Li, Q.; Xu, D. *Analyst* **2006**, *131*, 745−750.
(44) Dhayal, B.; Henne, W. A.; Doorneweerd, D. D.; Reifenberger, R. G.; Low, P. S. *J. Am. Chem. Soc.* **2006**, *128*, 3716−3721.

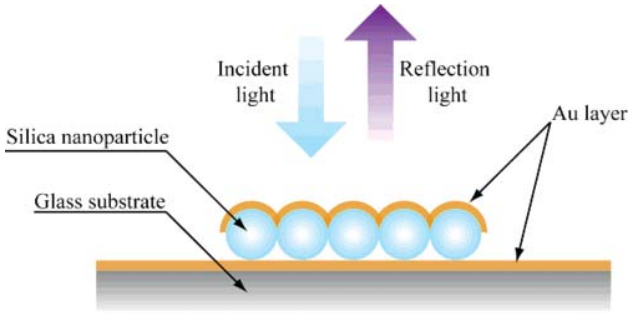

Figure 1. Construction of the multiarray LSPR-based nanochip. The surface modified silica nanoparticles were aligned onto the gold-deposited glass substrate surface. Subsequently, the gold layer was deposited onto the silica nanoparticle layer.

EXPERIMENTAL SECTION

Materials. Self-assembled monolayer (SAM) formation on the gold substrate surface was performed using 4,4′-dithiodibutyric acid (DDA) that was purchased from Aldrich. The activation of the carboxyl group of DDA was performed using 1-ethyl-3-(3-dimethylaminopropyl)carbodiimide (EDC) from Dojindo Laboratories (Kumamoto, Japan). Surface modification of silica nanoparticles employed 3-aminopropyltriethoxysilane (γ-APTES) from Shin-Etsu Chemical Co., Ltd. (Tokyo, Japan). Silica nanoparticles (particle diameter: 100 nm) for preparing the nanoparticle layer were purchased from Polysciences Inc. (Warrington, PA). Glass slide substrate (S-1111, 76 × 26 mm, thickness: ~0.8 to 1.0 mm) was purchased from Matsunami Glass Ind. Ltd. (Osaka, Japan). Electronic grade sulfonic acid and hydrogen peroxide for cleaning the glass slide substrates were purchased from Kanto Kagaku (Tokyo, Japan). *N*-Hydroxysuccinimide (NHS) for antibody immobilization was purchased from Wako Pure Chemical Industries, Ltd. (Osaka, Japan). The anti-immunoglobulin A (IgA), IgD, IgG, IgM, C-reactive protein (CRP), and fibrinogen antibodies were obtained from Cosmo Bio (Tokyo, Japan). Ultrapure water (18.3 MΩ-cm) from Millipore was used in all preparations.

Apparatus. For the deposition of gold and chromium layer on the glass slide substrate, a thermal evaporator (SVC-700TM/700-2) was purchased from Sanyu Electron Co., Ltd. (Tokyo, Japan). For monitoring of the base pressure, an analogue ionization vacuum gauge was utilized (GI-TL3, ULVAC, Kanagawa, Japan). The growth rate in thickness was monitored by a quartz crystal microbalance (QCM, model TM-200R, Maxtek, Inc., CA). The spectrophotometer (USB-2000-UV−vis, wavelength range: ~200 to 1100 nm), tungsten halogen light source (LS-1, wavelength range: ~360 to 2000 nm), and optical fiber probe bundle (R-200-7 UV−vis, fiber core diameter: 200 μm; wavelength range: ~250 to 800 nm), were purchased from Ocean Optics (Dunedin, U.S.A.). For spotting the sample solutions onto the chip surface, we used a nanoliter dispensing system (Shotmaster 300, 3-axis type) from Musashi Engineering, Inc. (Tokyo, Japan).

Preparation of the Multiarray LSPR-Based Nanochip. Our LSPR-based nanochip was constructed by a core−shell-structured nanoparticle layer (Figure 1). The surface-modified silica nanoparticle was used as the "core", and the "shell" was applied with the top and the bottom gold layers that were deposited using thermal deposition. For the preparation of the surface-modified silica nanoparticles, silica nanoparticles (particle diameter: 100 nm) were dried for 24 h at 55°C and reacted with 1% (v/v) γ-APTES solution in ultrapure water for 24 h at room temperature (RT) by stirring continuously. After the surface modification, the γ-APTES solution was removed in the centrifugal operation for 1 h at 3500 rpm, and the recovered nanoparticles were washed with ultrapure water. Both the washing and centrifugal operations were repeated three times, then surface-modified nanoparticles were dried for 5 min at 120°C. Silica nanoparticles modified with amino groups were thus obtained. Surface-modified nanoparticles were stored in the desiccator until use, then the colloid solution of the surface-modified silica nanoparticles was simply prepared by dispersing the desired amount in ultrapure water.

After the pretreatment of their surfaces, glass slides were used as substrates for the formation of the nanoparticle layer. All substrates were cleaned via a three-step process of ultrasonic cleaning in acetone for 30 min, soaking in a mixture of sulfuric acid and hydrogen peroxide (Piranha solution) at a ratio of 5:1 (v/v) for 30 min, followed by a thorough rinsing with ultrapure water, and drying at RT. Finally, the clean substrates were stored in a desiccator until use. (**Warning:** *Piranha solution is highly hazardous and reactive and may explode on coming into contact with organic solvents. Extreme precautions must be taken at all times.*)

A thermal evaporator was used at a base pressure of 8×10^{-6} Torr. The growth rate was monitored using QCM and manually adjusted to 1.0 Å/s. Gold and chromium with 99.99% purity was obtained from Furuya Metal (Tokyo, Japan). A chromium layer of 5 nm and the bottom gold layer of 40 nm were deposited onto the glass substrates. Additionally, after the formation of the silica nanoparticle monolayer, 30 nm of another gold layer was evaporated at the top.

For the fabrication of LSPR-based nanochip using surface-modified silica nanoparticles, 1 mM of DDA solution was introduced to the gold-deposited glass slide substrate surface, and the SAM was formed in 1 h. SAM functionalization was carried out with 400 mM EDC for 1 h. EDC activated the carboxyl groups of the DDA, and therefore, the amino groups of silica nanoparticles could form esters with the activated carboxyl groups. The surface-modified silica nanoparticles that were modified with amino groups (1% w/v) by silane coupling reagent in ultrapure water were exposed to the activated SAM-modified gold substrate surface for 1 h. The nanoparticle layer modified substrates were rinsed thoroughly with ultrapure water to remove the excess surface modified nanoparticles and dried at RT. During the preparation of the nanoparticle layer, a silicon chamber was attached onto the gold layer-deposited glass slide surface to control the spread of the sample solutions. Finally, a top gold layer (30 nm) was deposited onto the nanoparticle layer modified substrates using the thermal evaporator (Figure 2a). After these fabrication procedures, the LSPR band was monitored in the visible range. The multiarray (20 mm × 60 mm) of core−shell structured nanoparticle layer substrate could thus be obtained (Figure 2b).

Immobilization of Antibodies onto Multiarray LSPR-Based Nanochip. The antibody immobilization onto the multiarray LSPR-based nanochip surface was carried out in a similar fashionwith the formation of a nanoparticle monolayer (Figure 3a). DDA at 1 mM was introduced to the LSPR-based biochip surface, and a SAM was formed in 1 h. SAM functionalization was carried

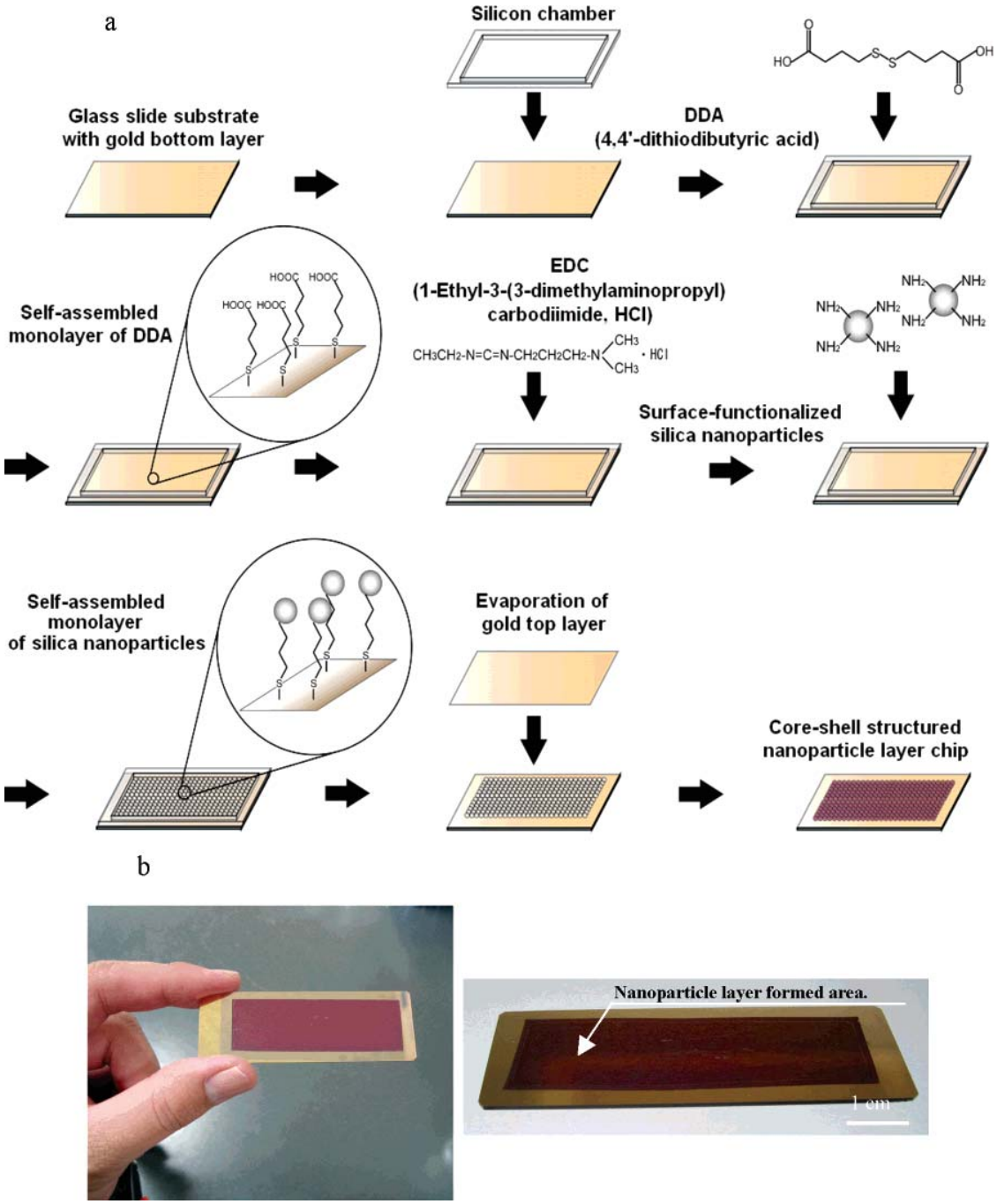

Figure 2. Fabrication procedure and photograph of the multiarray LSPR-based nanochip. (a) Fabrication procedure of the multiarray LSPR-based protein array biochip. (b) Photograph of the multiarray gold-capped nanoparticle layer substrate. The antibodies were immobilized onto the multiarray gold-capped nanoparticle layer substrate surface using a nanoliter dispensing system.

out with 400 mM EDC for 1 h, and then 100 mM NHS solution was added to the SAM-functionalized surface for 1 h. Protein A at 100 μg/mL was immobilized on the surface for 1 h, which reacted with the Fc region of the IgG antibodies. Antibodies against IgA, IgD, IgG, IgM, CRP, and fibrinogen at 100 μg/mL were spotted onto the protein A-modified surfaces using the nanoliter dispensing system at a volume of 100 nL (Figure 3b) and incubated for 1 h. Finally, the antibody-immobilized surface was rinsed thoroughly with 20 mM phosphate buffered saline (PBS, pH 7.4) and dried at RT. In total, 300 antibody-immobilized spots were formed on the chip surface.

Label-Free Detection of the Proteins Using the LSPR-Based Nanochip. After the immobilization of the antibodies on the multiarray chip, different concentrations of antigen solutions (~0 to 100 μg/mL) were introduced onto the 300 spots using the nanoliter dispensing system and incubated for 30 min (Figure 3c). Especially, the total sample volume was significantly reduced. Each spot was reacted with a sample solution of 100 nL containing the antigens at varying concentrations. After an incubation period of 30 min, a stringent washing procedure with 1% (v/v) Tween-20 was applied to suppress the nonspecific adsorption. Subsequently, evaluation of the optical characteristics of the chip was

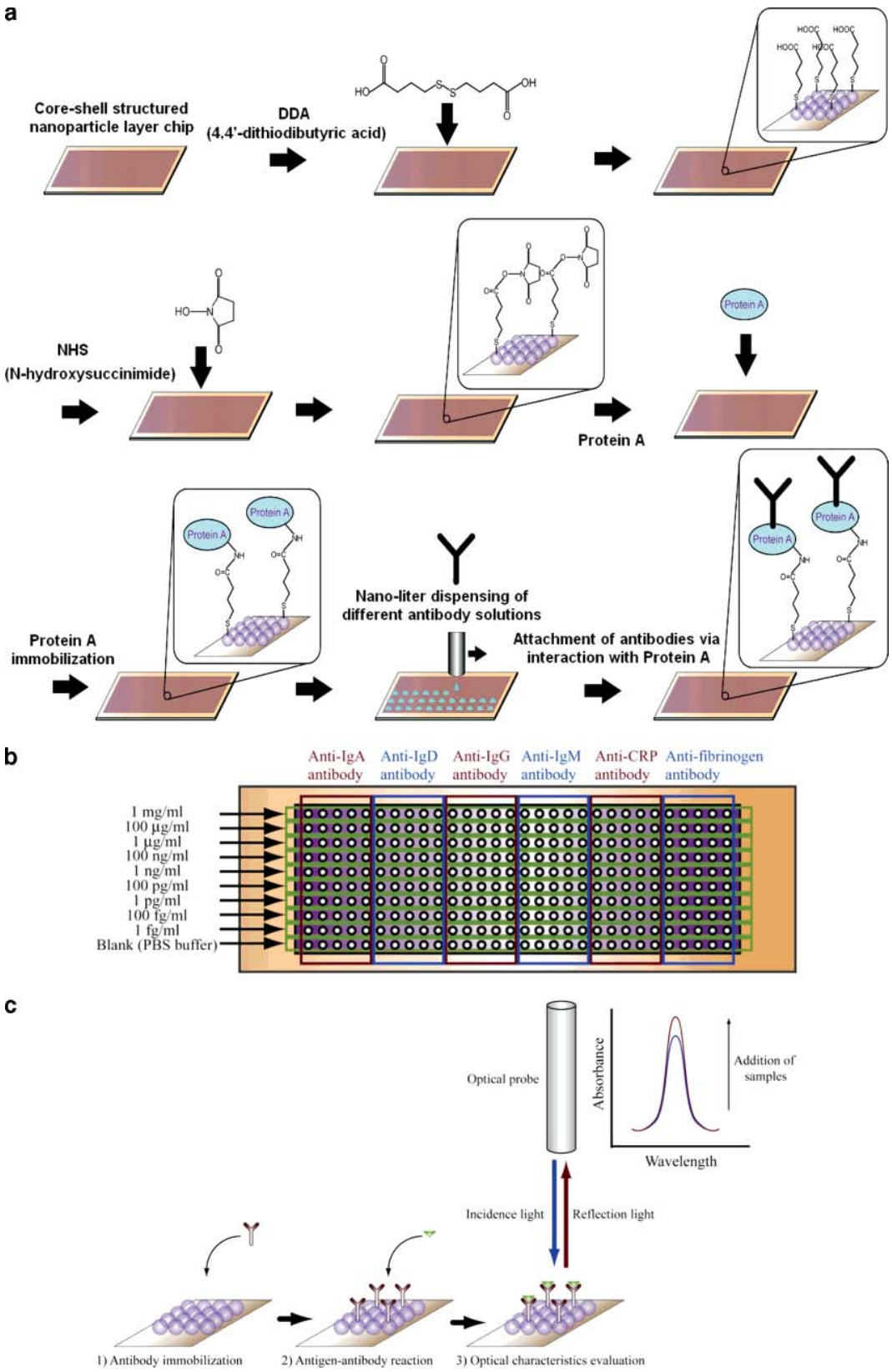

Figure 3. Experimental conditions of the multiarray LSPR-based nanochip. (a) Immobilization of antibodies on the surface of the multiarray LSPR-based protein array biochip surface. (b) Construction of the antibody immobilized spots and antigen concentrations. Six kinds of antibodies and antigens were spotted onto the multiarray LSPR-based nanochip surface. (c) Experimental setup of the multiarray LSPR-based nanochip.

carried out. All absorbance spectra were taken from a range of 400−800 nm on the UV−vis spectrometer at RT. White light emerging from the optical fiber bundle was incident onto the nanochip from the vertical direction. The reflected light was

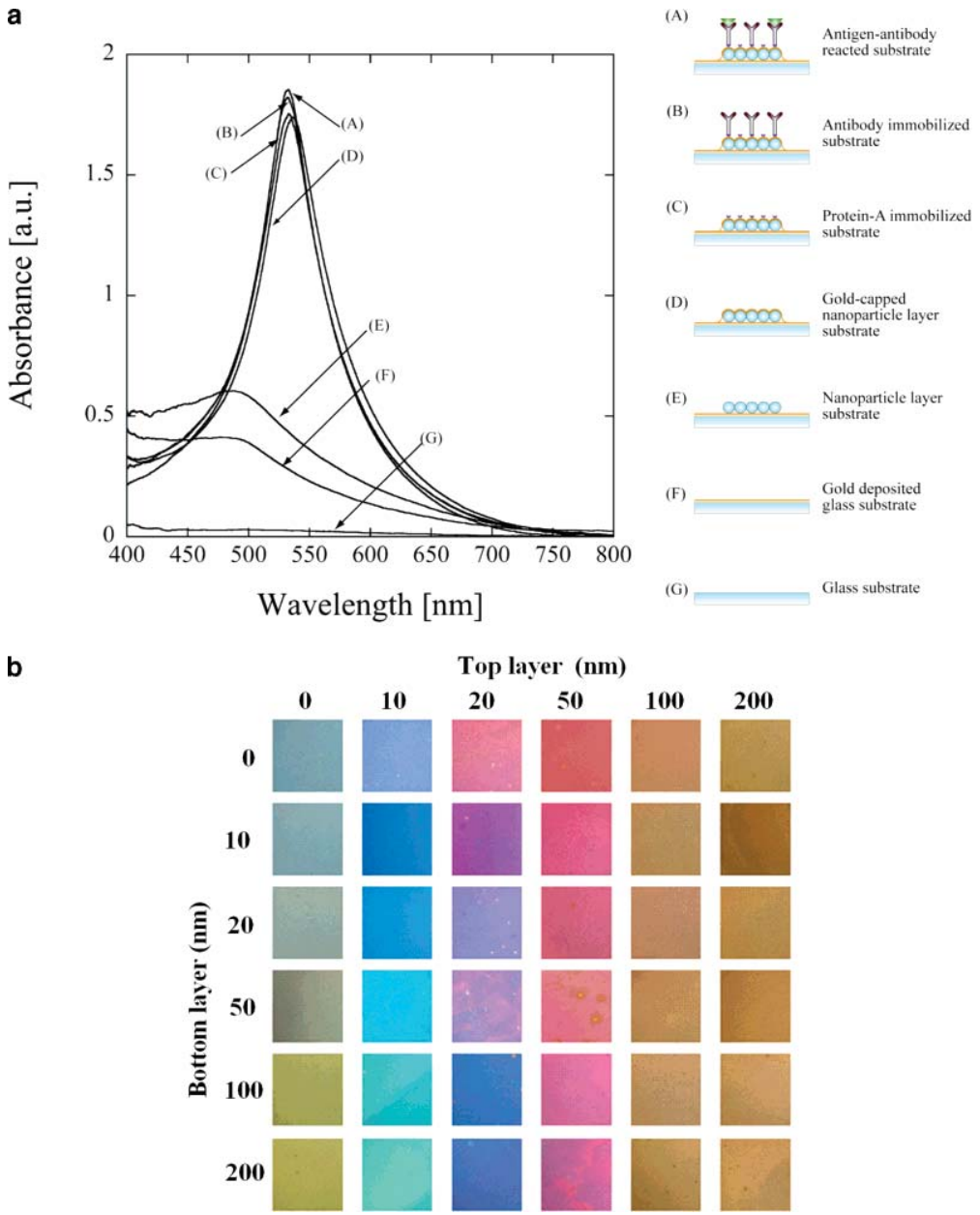

Figure 4. (a) Optical characteristics of the LSPR-based nanochip. The specific LSPR absorbance peak was observed after the deposition of the top gold layer at step D. (b) Optical images of the LSPR-based nanochips that were fabricated using different thicknesses of the top and bottom gold layers.

coupled into the detection fiber probe of the optical fiber bundle and analyzed by the UV−vis spectrometer. The evaluation of the results obtained from the nanochip surface revealed that the specific absorbance strength change was directly related to the applied antigen concentration on the spot.

RESULTS AND DISCUSSION

Optical Characteristics of the Multiarray LSPR-Based Nanochip. The optical characteristics of the LSPR-based nanochip using noble metal nanoparticles or metal nanoislands were discussed with the help of a shift in the absorbance peak wavelength;[29,34] however, we observed a significant increase in the absorbance strength using our LSPR-based nanochip (Figure 4a). Similarly, the increase in the intensity at the peak wavelength along with the increasing layer thickness was reported previously.[37,38] The absorbance peak of our nanochip was also observed at ~520 nm. The optical characteristics of our core−shell-structured nanoparticle layer substrate could be obtained easily with more efficiency than the conventional biochips, which employ the noble metal nanoparticles immobilized on the solid substrate. The conventional LSPR-based nanochips face complicated procedures during the synthesis of the metal nanoparticles with a uniform size and their immobilization as a monolayer onto the solid substrate surface. However, our LSPR-based nanochip is easy to fabricate with the self-assembly of surface-functionalized silica nanoparticles and the subsequent gold deposition onto them. The optical characteristics, such as peak wavelength of our nanochip, were

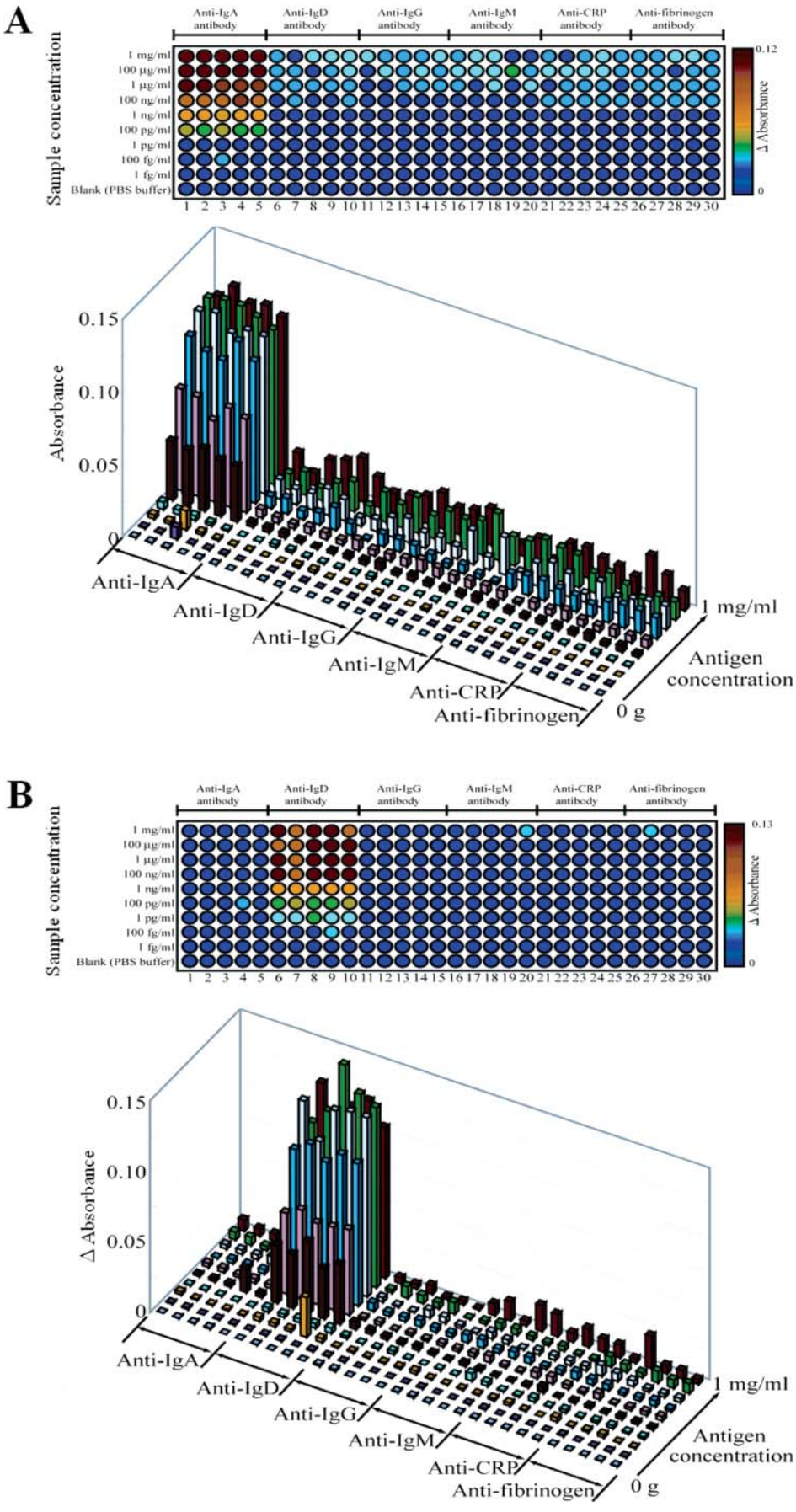
A
Anti-IgA antibody
Anti-IgD antibody
Anti-IgG antibody
Anti-IgM antibody
Anti-CRP antibody
Anti-fibrinogen antibody
Sample concentration
1 mg/ml
100 µg/ml
1 µg/ml
100 ng/ml
1 ng/ml
100 pg/ml
1 pg/ml
100 fg/ml
1 fg/ml
Blank (PBS buffer)
1 2 3 4 5 6 7 8 9 10 11 12 13 14 15 16 17 18 19 20 21 22 23 24 25 26 27 28 29 30
0.12
Δ Absorbance
0
Absorbance
0.15
0.10
0.05
0
Anti-IgA
Anti-IgD
Anti-IgG
Anti-IgM
Anti-CRP
Anti-fibrinogen
1 mg/ml
Antigen concentration
0 g
B
Anti-IgA antibody
Anti-IgD antibody
Anti-IgG antibody
Anti-IgM antibody
Anti-CRP antibody
Anti-fibrinogen antibody
Sample concentration
1 mg/ml
100 µg/ml
1 µg/ml
100 ng/ml
1 ng/ml
100 pg/ml
1 pg/ml
100 fg/ml
1 fg/ml
Blank (PBS buffer)
1 2 3 4 5 6 7 8 9 10 11 12 13 14 15 16 17 18 19 20 21 22 23 24 25 26 27 28 29 30
0.13
Δ Absorbance
0
Δ Absorbance
0.15
0.10
0.05
0
Anti-IgA
Anti-IgD
Anti-IgG
Anti-IgM
Anti-CRP
Anti-fibrinogen
1 mg/ml
Antigen concentration
0 g

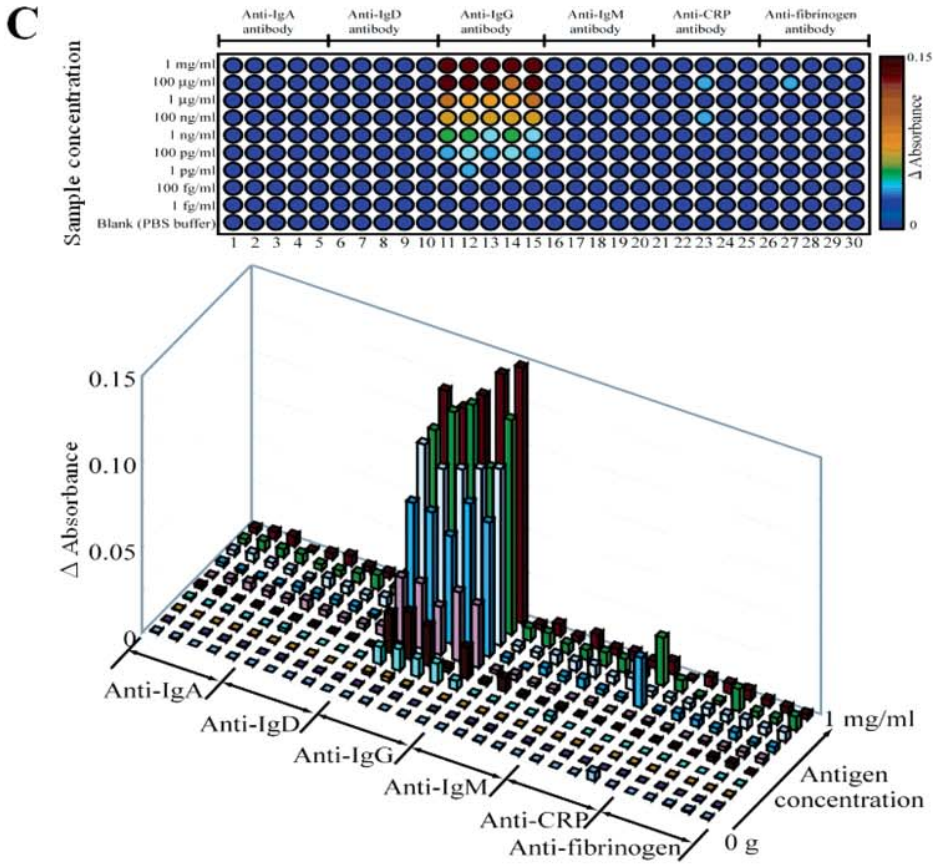
C
Anti-IgA antibody
Anti-IgD antibody
Anti-IgG antibody
Anti-IgM antibody
Anti-CRP antibody
Anti-fibrinogen antibody
Sample concentration
1 mg/ml
100 µg/ml
1 µg/ml
100 ng/ml
1 ng/ml
100 pg/ml
1 pg/ml
100 fg/ml
1 fg/ml
Blank (PBS buffer)
1 2 3 4 5 6 7 8 9 10 11 12 13 14 15 16 17 18 19 20 21 22 23 24 25 26 27 28 29 30
0.15
Δ Absorbance
0
0.15
0.10
0.05
Δ Absorbance
0
Anti-IgA
Anti-IgD
Anti-IgG
Anti-IgM
Anti-CRP
Anti-fibrinogen
1 mg/ml
Antigen concentration
0 g

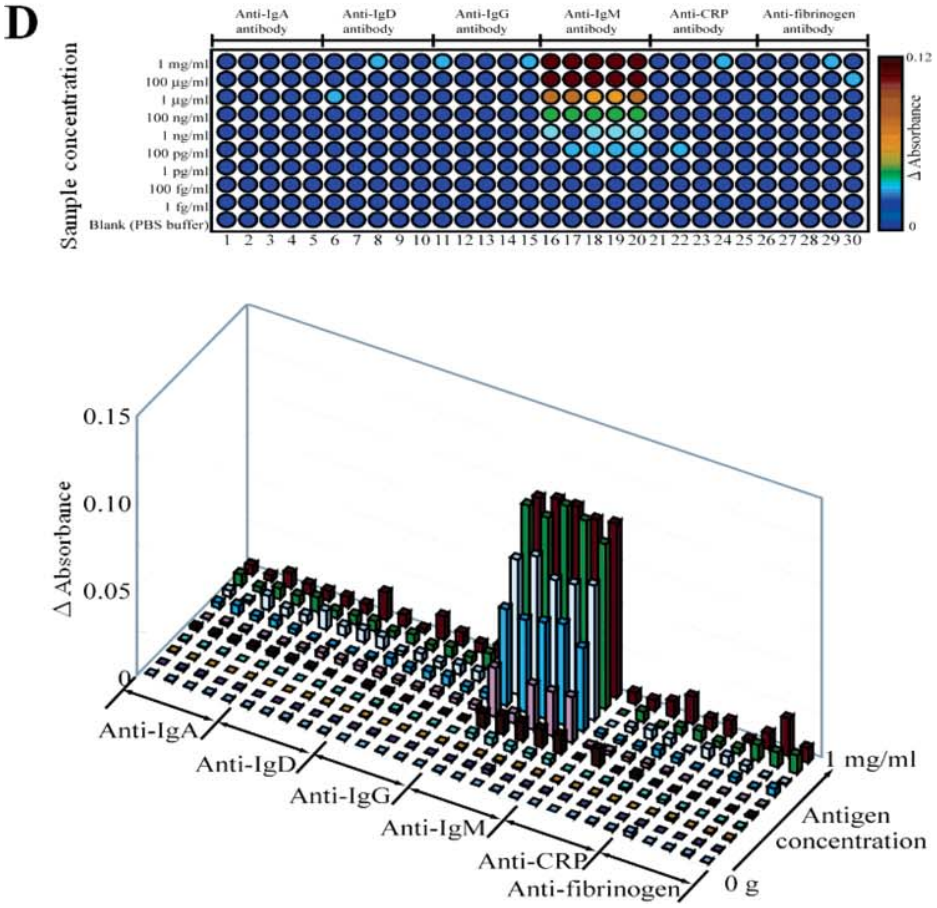
D
Anti-IgA antibody
Anti-IgD antibody
Anti-IgG antibody
Anti-IgM antibody
Anti-CRP antibody
Anti-fibrinogen antibody
Sample concentration
1 mg/ml
100 µg/ml
1 µg/ml
100 ng/ml
1 ng/ml
100 pg/ml
1 pg/ml
100 fg/ml
1 fg/ml
Blank (PBS buffer)
1 2 3 4 5 6 7 8 9 10 11 12 13 14 15 16 17 18 19 20 21 22 23 24 25 26 27 28 29 30
0.12
Δ Absorbance
0
0.15
0.10
0.05
Δ Absorbance
0
Anti-IgA
Anti-IgD
Anti-IgG
Anti-IgM
Anti-CRP
Anti-fibrinogen
1 mg/ml
Antigen concentration
0 g

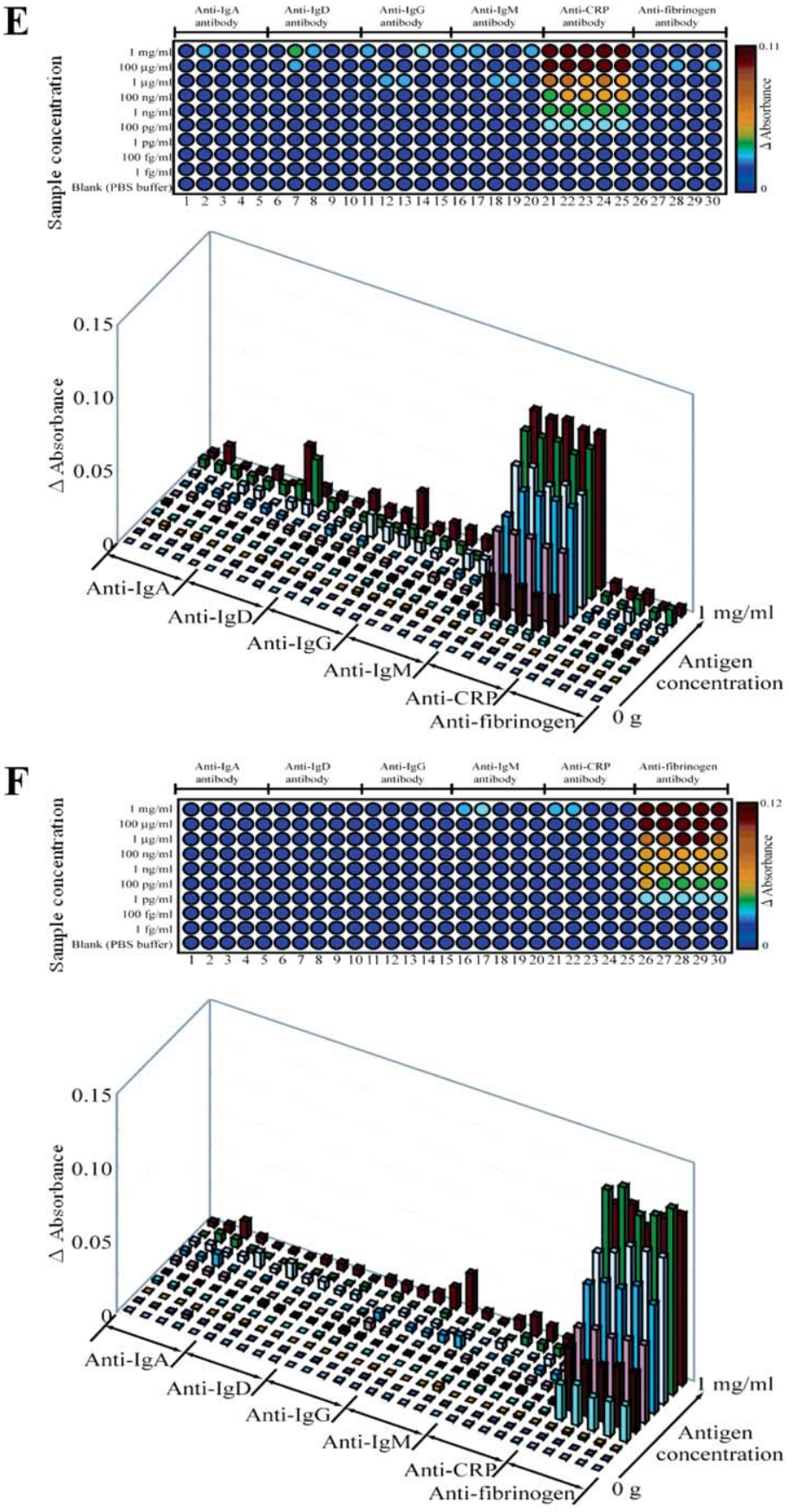

Figure 5. Absorbance measurements at each spot using the multiarray LSPR-based nanochip. After the introduction of antigens at different concentrations using the nanoliter dispensing system, the LSPR spectra were recorded for (A) immunoglobulin A (IgA), (B) IgD, (C) IgG, (D) IgM, (E), C-reactive protein (CRP), and (F) fibrinogen.

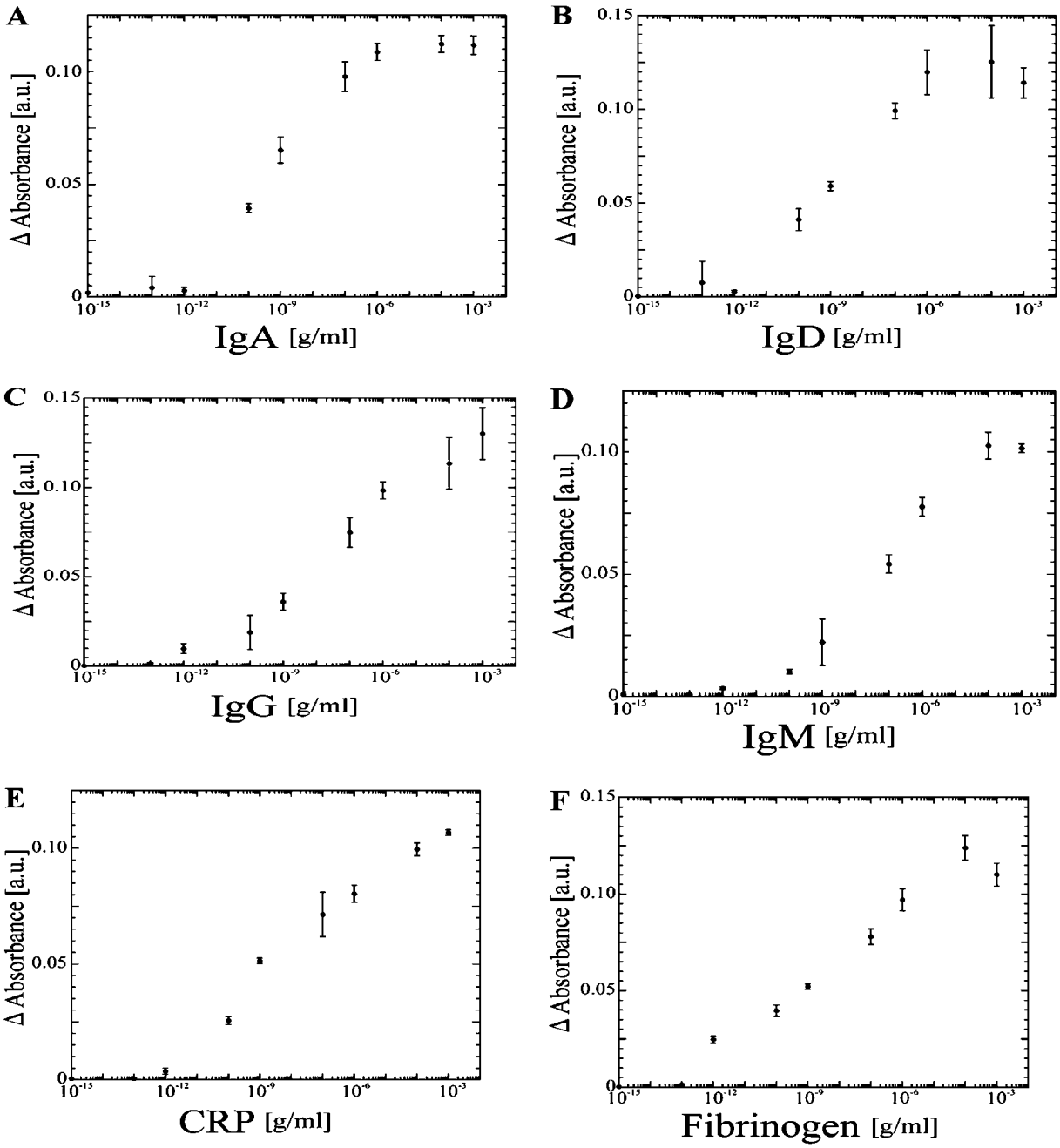

Figure 6. Calibration curves for the proteins on the multiarray LSPR-based nanochip.

greatly influenced by the thickness of the top and bottom gold layers (Figure 4b). The visual color change on the nanochip surface indicated the changes in the peak wavelength of the LSPR spectra (Figure 4b). Upon observation of similar optical characteristics, we determined that our gold-capped nanoparticle layer substrate had properties similar to that of the nanoshell-structured nanoparticles. Moreover, the peak wavelength could easily be controlled for the excitation of LSPR using our core−shell-structured nanoparticle layer substrates.

Multiple Detection of Proteins Using Multiarray LSPR-Based Nanochip. The antibody solutions were spotted on the multiarray LSPR-based nanochip surface using a nanoliter dispensing system. In this research, a total of 300 antibody-immobilized spots were prepared on the nanochip surface by dispensing six different antibodies. Each antibody was dispensed onto 50 predetermined spots. Additionally, each spot was separated with a pitch of 1 mm to prevent cross-contamination. LSPR spectra were measured after incubation with the different concentrations of antigens for 30 min, then the washing procedure was carried out as described in the Experimental Section. The absorbance strength change was recorded depending on the concentration of the antigens, immunoglobulin A (IgA), IgD, IgG, IgM, C-reactive protein (CRP), and fibrinogen, as shown in Figure 5A−F, respectively. The multiarray LSPR-based nanochip provided a limit of detection of 100 pg/mL for all of the proteins, as shown in Figure 6. The wide detection range of our nanochips was linear

up to 1 μg/mL. Our method using multiarray LSPR-based nanochip is a promising candidate for low-cost and highly sensitive detection of multiple analytes in a simple and rapid format.

CONCLUSIONS

Future trends in diagnostics will continue in miniaturization of biochip technology toward nanoscale. Our multiarray LSPR-based nanochip provides a convenient, low-cost, and label-free method for specific and highly sensitive detection of the biomolecular interactions in a parallel format. We anticipate that this technology will extend the limits of current molecular diagnostics and enable point-of-care diagnosis as well as promote the development of personalized medicine. The multiparallel possibilities of biosensing applications have the potential to allow the optimization of biomarker research, cancer diagnosis, and also the detection of infectious microorganisms for biodefense. Especially, the cost for the fabrication of our multiarray LSPR-based nanochip, including the optical apparatus, is significantly lower than that of a conventional SPR system. This LSPR method is "easy to operate" even by "nonspecialists". The LSPR-based multiarray nanochip presents a highly versatile method that is readily applicable to the other kinds of bioassays, such as metabolomics and cellomics.

ACKNOWLEDGMENT

The authors thank Dr. Shohei Yamamura, Dr. Masato Saito, and Dr. Yasutaka Matsubara from the Japan Advanced Institute of Science and Technology (JAIST) and Dr. Takeshi Hatsuzawa and Dr. Yasuko Yanagida from the Tokyo Institute of Technology for valuable advice during the monitoring of the large number of antigen-antibody reactions. The authors also thank Musashi Engineering, Inc. for providing the nanoliter dispensing system.

Received for review May 5, 2006. Accepted June 10, 2006.

AC0608321